IJMMM International Journal of Minerals, Metallurgy and Materials 矿物冶金与材料学报（英文版）

Controlled crystal orientation of two-dimensional Ruddlesden–Popper halide perovskite films for solar cells

Jiuyao Du, Mengqi Zhang, and Jianjun Tian

Cite this article as:
Jiuyao Du, Mengqi Zhang, and Jianjun Tian, Controlled crystal orientation of two-dimensional Ruddlesden–Popper halide perovskite films for solar cells, *Int. J. Miner. Metall. Mater.*, 29(2022), No. 1, pp. 49-58. https://doi.org/10.1007/s12613-021-2341-z

View the article online at SpringerLink or IJMMM Webpage.

International Journal of Minerals, Metallurgy and Materials
Volume 29, Number 1, January 2022, Page 49
https://doi.org/10.1007/s12613-021-2341-z

Invited Review

Controlled crystal orientation of two-dimensional Ruddlesden–Popper halide perovskite films for solar cells

Jiuyao Du[*], *Mengqi Zhang*[*], *and Jianjun Tian*[✉]

Beijing Advanced Innovation Center for Materials Genome Engineering, Institute for Advanced Materials and Technology, University of Science and Technology Beijing, Beijing 100083, China

(Received: 4 April 2021; revised: 14 August 2021; accepted: 17 August 2021)

Abstract: Metal halide perovskite solar cells have attracted considerable attention because of their high-power conversion efficiency and cost-effective solution-processable fabrication; however, they exhibit poor structural stability. Two-dimensional (2D) Ruddlesden–Popper (RP) perovskites could address the aforementioned issue and present excellent stability because of their hydrophobic organic spacer cations. However, the crystallographic orientation of 2D crystals should be perpendicular to the bottom substrates for charges to transport fast and be collected in solar cells. Moreover, controlling the crystallographic orientation of the 2D RP perovskites prepared by the solution process is difficult. Herein, we reviewed the progress of recent research regarding 2D RP perovskite films with the focus on the crystallographic orientation mechanism and orientation controlling methods. Furthermore, the current issues and prospects of 2D RP perovskites in the photovoltaic field were discussed to elucidate their development and application in the future.

Keywords: two-dimensional; Ruddlesden–Popper; crystallographic orientation; perovskite solar cells

1. Introduction

Organic–inorganic halide perovskite solar cells (PSCs) have attracted increasing research interest owing to their exceptionally excellent optoelectronic properties, such as high absorption coefficient, low exciton binding energy, fast carrier mobility, and long charge carrier diffusion length [1−13]. In 1978, the structure of organic–inorganic hybrid perovskite $CH_3NH_3PbX_3$ ($MAPbX_3$, X = Cl, Br, and I) materials was reported for the first time [14]. In 2009, these materials were applied as dye sensitizers to fabricate dye-sensitized solar cells (DSCs) with a power conversion efficiency (PCE) of 3.8% [15]. However, the stability of these solar cells was poor because of the use of liquid electrolytes. In 2012, solid-state solar cells based on methylammonium lead iodide perovskite films ($CH_3NH_3PbI_3$, $MAPbI_3$) with a higher PCE of 9.7% and better stability than DSC-type devices were fabricated [16]. Because of intensive studies conducted on perovskite materials and their photovoltaic devices, the PCE of state-of-the-art PSCs has been increased to more than 25% within ten years. Nevertheless, the poor structural stability and ion migration of PSCs can deteriorate their performance during the operation process [17−21], thereby limiting their further development and commercial application. Recent studies have shown that hydrophobic organic spacer cations could be introduced into three-dimensional (3D) perovskites to form two-dimensional (2D) perovskites. The hydrophobic organic spacer cations in 2D perovskites can block the invasion of water molecules to improve structural stability and restrain ion migration. Moreover, these stable 2D perovskite layers can be deposited on the top of 3D perovskite films to improve their structural stability and passivate surface defects [22−28].

2D perovskites in metal halide PSCs have two main structures, namely, Ruddlesden–Popper (RP) and Dion–Jacobson (DJ) phases [29−35]. 2D RP perovskites are commonly used in the photovoltaic field [36−42]. In 1957, Ruddlesden and Popper [43] first investigated the compounds with K_2NiF_4-type structure which was similar to the perovskite structure. Since then, 2D perovskites with this structure have been called 2D "Ruddlesden–Popper" perovskites. The 2D RP perovskite structure can be regarded as a sandwich structure that the perovskite octahedron layer locates between two organic spacer cations, which results in excellent structural and environmental stability [44−48] and migration suppression [49]. In 2014, the 2D RP perovskite $(PEA)_2(MA)_2Pb_3I_{10}$ (PEA: phenethylammonium, $C_6H_5(CH_2)_2NH_3^+$) was first utilized to construct solar cells with a PCE of 4.73% [44]. This type of 2D RP PSCs exhibited remarkable humidity stability, which was better than that of $MAPbI_3$-based solar cells. Currently, the PCE of state-of-the-art 2D RP PSCs is more than 18% [50−53], which is close to that of conventional 3D

*These authors contributed equally to this work.

✉ Corresponding author: Jianjun Tian E-mail: tianjianjun@mater.ustb.edu.cn

PSCs. However, some challenges still inhibit the development of 2D RP PSCs. For example, the growth orientation of 2D layered perovskites is random, and depends on the thermodynamics and kinetics of materials. Some randomly aligned 2D crystals significantly worsen the photovoltaic performance of solar cells. In particular, if the growth orientation of 2D RP perovskites is parallel to the substrate, the charge transfer in devices will be reduced because of the low conductivity of organic spacer cations. In this case, the preferred orientation of the 2D RP perovskites should be vertically aligned to the substrates to enhance the charge transport capability and obtain smooth and surface-averaged films. Overall, controlling the crystallographic orientation of 2D RP perovskites is important to obtain high-performance solar cells.

In this review, we summarized the research studies of the crystallographic orientation of 2D RP PSCs from aspects of the fabrication process, composition, and solvent engineering. We also outlined the perspectives toward the molecular structure design of organic spacer cations, phase distribution, and mixed phase of 2D RP perovskites for high-performance photovoltaic devices.

2. Structures and characteristics of 2D RP perovskites

2.1. Structure of 2D RP perovskites

The 2D RP perovskite structure comprises large organic spacer cations and octahedral units [54−57]. The perovskite octahedral layer is sandwiched between organic spacer cations on both sides. The general structural formula of 2D RP perovskites is $A'_2A_{n-1}B_nX_{3n+1}$ (n = 1, 2, 3, 4, …), where A′ is an aliphatic or aromatic organic ammonium cation containing one amino group, e.g., $CH_3(CH_2)_3NH_3^+$ (*n*-butylammonium, BA) or $C_6H_5(CH_2)_2NH_3^+$; A is an organic or inorganic cation, e.g., $CH_3NH_3^+$, $CH(NH_2)_2^+$, or Cs^+; B is a metal cation, e.g., Pb^{2+} and Sn^{2+}; X is a halogen anion, e.g., Cl^-, Br^-, or I^-; and n is the number of $[BX_6]^{4-}$ octahedral layers. The 2D RP perovskite crystal structure can be regarded as n $[BX_6]^{4-}$ octahedral layers locate between two layers of organic spacer cations (Fig. 1(a)). The organic spacer cations between two adjacent layers are connected by van der Waals forces [58]. The inorganic layer acts as a "well," whereas the organic layer acts as a "barrier" to form a natural multiple quantum well structure [59]. The n value is related to the material phase. With the increase of the n value, the perovskite phase transforms from 2D to quasi-2D and eventually to 3D (the n value approaches infinity) [55]. The n values can be controlled by adjusting the composition stoichiometry of the precursor, which considerably affects the optoelectronic properties of 2D RP films. As shown in Fig. 1(b), the large organic spacer cations can block the invasion of water molecules, resulting in stable 2D RP perovskites. In contrast, the organic spacer cations can suppress carrier transport, thereby inhibiting ion migration and reducing the decomposition process of perovskites. All of the aforementioned parameters are critical for the power conversion performance of PSCs. Because of the structure of perovskite materials, the perpendicular growth orientation of 2D RP perovskite crystals is favorable for charges to transport to the electron or hole transport layer along the Pb−I−Pb pathway, thereby improving the optoelectronic performance of solar cells [54].

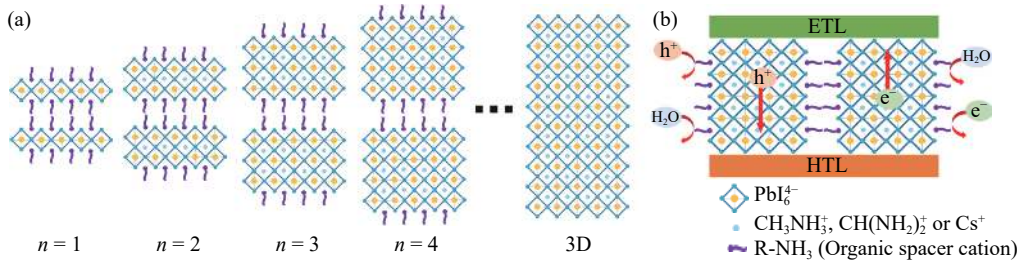

Fig. 1. Schematic illustration of (a) the crystal structures of 2D RP perovskite and (b) the electron, hole, and water molecule transmission path. ETL—Electron transport layer; HTL—Hole transport layer.

2.2. Crystallographic orientation of 2D RP perovskite

The growth orientation of the 2D RP perovskite phase not only depends on the orientation of the initial crystal nucleus but is also affected by the growth rate and initial crystal nuclei density. A slow growth rate and a small initial density are preferable for the formation of oriented 2D RP perovskite films. Non-oriented, parallel, and perpendicular are three crystallographic orientation types of 2D RP perovskite films [60]. The non-oriented growth of perovskites results in random and non-preferred crystals. The parallel growth of perovskites (Fig. 2(a)) means that the growth direction of the $[B_nX_{3n+1}]^{(1+n)-}$ planes is parallel to the substrate because of the separation effect of organic spacer cations. The perpendicular growth of perovskites (Fig. 2(b) and (c)) means that the growth direction of the $[B_nX_{3n+1}]^{(1+n)-}$ planes is perpendicular to the substrate. The growth orientation of the 2D RP perovskite phase with a small n value tends to be parallel to the substrate. When the n value increases, the perovskite phase is preferentially perpendicular to the substrate. According to a previous report [61], the nuclei of 2D RP perovskites are initially formed at the liquid–air interface, affecting the crystal growth and orientation. Fig. 2(d) shows two preferred orientations of the initial nucleation at the liquid–air interface. From the perspective of structural stability, the initial nucleus with vertical orientation (Scenario 1) is more stable than the initial nucleus with horizontal orientation (Scenario 2). The growth orientation has a considerable effect on the distri-

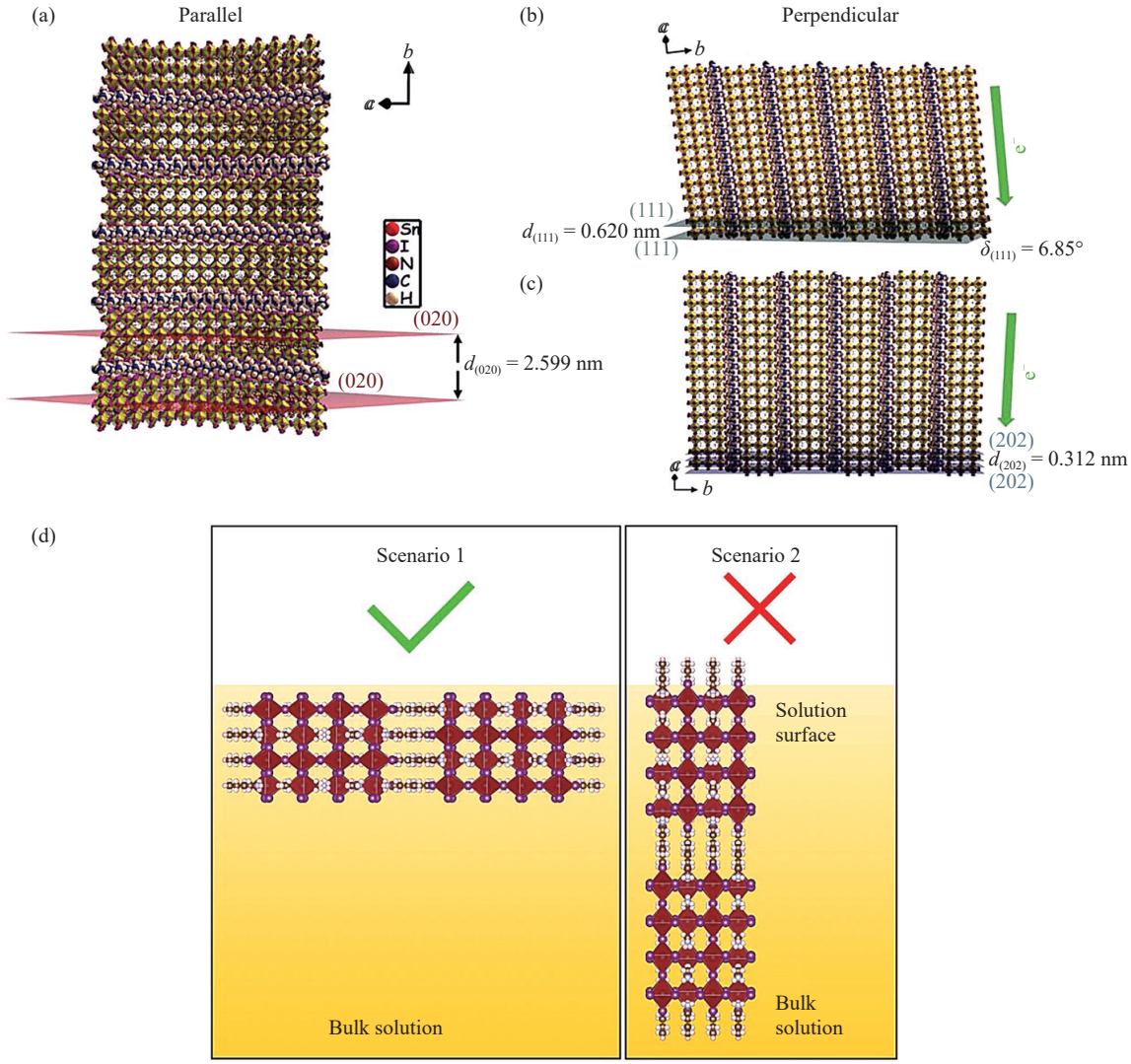

Fig. 2. 2D $(BA)_2(MA)_2Sn_3I_{10}$ perovskite: (a) (0*k*0) parallel orientation, (b) (111) nearly perpendicular orientation, and (c) (202) perfectly perpendicular orientation. Reprinted with permission from Ref. [60]. Copyright 2017 American Chemical Society. (d) Schematics of the preferred orientation at the liquid–air interface. The two possible nucleus orientations at the anisotropic precursor solution–air interface are shown in Scenarios 1 and 2. Reprinted by permission from Spring Nature: *Nat. Commun.*, Origin of vertical orientation in two-dimensional metal halide perovskites and its effect on photovoltaic performance, A.Z. Chen, M. Shiu, J.H. Ma, M.R. Alpert, D.P. Zhang, B.J. Foley, D.M. Smilgies, S.H. Lee, and J.J. Choi, Copyright 2018.

bution of long-chain organic cations and $[BX_6]^{4-}$ octahedral layers. The vertical orientation of the initial nucleation induces perovskite vertical growth. Notably, this formation mechanism can be applied to any substrate material of PSCs. The formation mechanism of 2D RP perovskite with high orientation is also related to the cation solubility of the precursor solution [38]. The low solubility of organic halogen compounds (e.g., CH_3NH_3I) causes the nucleation of the 3D-like perovskite phase to an out-of-plane (111) orientation. Then, the 2D RP perovskite phase starts nucleating and growing by increasing the concentration of organic cations. Thus, the 2D RP perovskite film is composed of a gradient of *n* value perovskite phase.

3. Fabrication approaches for controlling the orientation of 2D RP perovskites

The preparation process directly affects the growth orientation and quality of 2D RP perovskite films. For the one-step method, 2D RP perovskite films are usually prepared by spin-coating a certain molar ratio of the precursor solution onto the substrates, which is similar to the preparation of 3D perovskite films. The films are easily obtained using this method, but exhibit poor performance because of the random growth orientation of the 2D RP perovskite phase in the film [44]. The internal charge transfer of the device is hindered by random crystals, resulting in a low short-circuit current density. To promote the nucleation of perovskite and improve the crystal orientation, an anti-solvent [62−66] is used to extract the solvent of the precursor solution during the spin-coating process. In this case, the gas–liquid interface rapidly reaches a supersaturated state. Then, the 2D RP perovskite phase begins to form nuclei. Owing to thermodynamic and dynamic stability, 2D RP perovskite nuclei with vertical substrate orientation form at the gas–liquid interface. These crystal nuclei act as seeds to induce the vertical growth of 2D RP per-

ovskite. Moreover, the anti-solvent with organic salts can induce the vertical growth of crystals to boost the formation of the 2D RP perovskites with vertical growth orientation [67]. Organic salts can also passivate the surface defects of 2D RP perovskites to reduce the nonradiative recombination. However, the anti-solvent method is harmful to the environment because of the volatilization of a large amount of organic solvent.

The hot-casting method can accelerate the evaporation speed of perovskite precursors to avoid the use of the anti-solvent [68−73]. In this method, the substrate is heated at a temperature higher than that of perovskite crystallization before spin-coating. The hot substrate promotes the volatilization of solvent and prolongs the crystal growth [70]. The 2D RP perovskite films prepared using this method could avoid the issues of the use of anti-solvent and random orientation of crystal growth [74]. Crystals with random growth orientation are easily formed in 2D RP films that are prepared with the room temperature casting method. Fig. 3(a) shows the diffraction ring of the 2D RP film obtained using the room temperature casting method, indicating the randomness of the domain orientation of the polycrystalline films. Meanwhile, the 2D RP film prepared using the hot-casting method exhibits sharp and discrete Bragg spots (Fig. 3(b)), indicating the preferred vertical growth orientation during perovskite crystallization. As shown in Fig. 3(c), the $(\bar{1}1\bar{1})$ and (202) spots indicate the vertical growth orientation. This arrangement of the growth orientation is also beneficial for the formation of highly uniform and well-crystallized layered perovskite films, thereby enhancing the charge transport capability. According to previous research, there is a large transformation energy barrier from the intermediate phase to the 2D RP

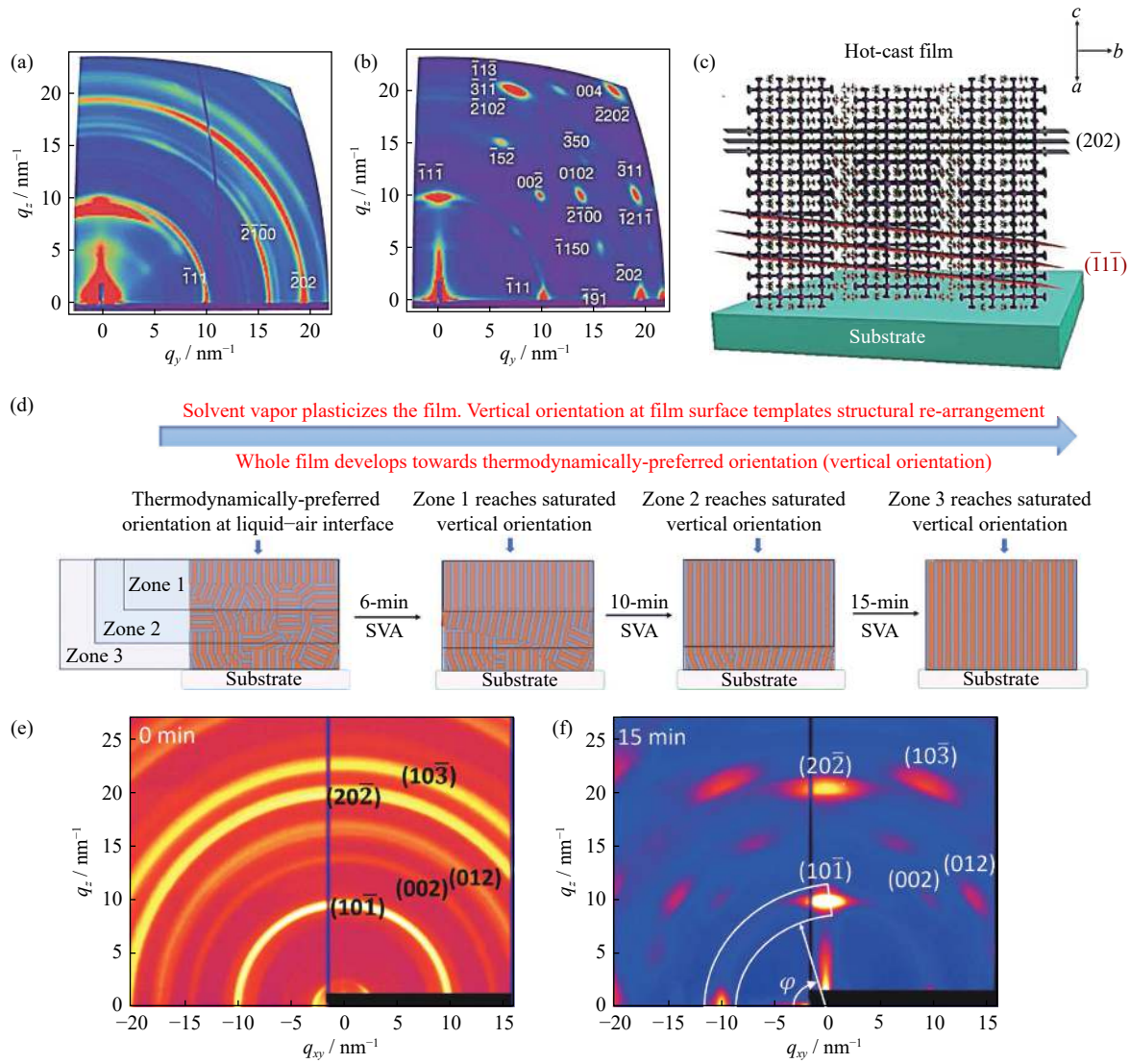

Fig. 3. Grazing-incidence wide-angle X-ray scattering maps of 2D RP perovskite films prepared using (a) room temperature casting and (b) hot casting. (c) Schematic representation of the (101) orientation, along with the $(\bar{1}1\bar{1})$ and (202) planes of a 2D perovskite crystal. q_{xy} and q_z are the scattering vectors perpendicular to and along the sample plane, respectively. (a−c) Reprinted by permission from Spring Nature: *Nature*, High-efficiency two-dimensional Ruddlesden-Popper perovskite solar cells, H. Tsai, W.Y. Nie, J.C. Blancon, *et al.*, Copyright 2016. (d) Illustration of the reorientation process during solvent vapor annealing. Structural evolution of perovskite thin films after SVA treatment. GIWAXS patterns of 2D RP perovskite films (e) before and (f) after SVA treatment. (d−f) Reprinted with permission from Ref. [80]. Copyright 2020 American Chemical Society.

monolayer [75−76]. The high-temperature substrate in the hot-casting method reduces the energy barrier and promotes the conversion of the intermediate phase into perovskite phase [77]. The preferential growth orientation of the 2D RP film obtained via hot casting can be attributed to the reduced surface energy or fast evaporation rate of the solvent. The hot-casting method is effective for improving the crystallinity, crystal growth, and orientation of perovskite films; however, it exhibits low repeatability.

Besides the conventional spin-coating and hot-casting methods, other methods have also been used to fabricate 2D RP perovskite films. The evaporation rate of the solvent affects the phase distribution and growth orientation of 2D RP perovskite films [78]. The slow solvent evaporation process is beneficial for the formation of vertical growth orientation nucleation at the gas–liquid interface. Vacuum poling is a method of vacuum treatment for the annealing process to control and ensure a uniform phase distribution with different n values [79]. A solvent vapor annealing (SVA) strategy was recently proposed to achieve the preferred vertical orientation of 2D RP perovskites [80]. The mechanism of the SVA strategy reorganizes the structure before forming the film. This method could be understood that the vertical growth orientation of the crystals is induced by the solvent vapor at the surface, which results in the vertical growth of the crystal from top to bottom (Fig. 3(d)). As shown in Fig. 3(e) and (f), 2D RP perovskite films exhibit the preferred growth orientation after SVA treatment. Notably, no impurity phases in 2D RP films are present after the SVA process, which enables the growth of perovskite grains.

4. Composition for controlling the orientation of 2D RP perovskites

4.1. Additives

The additives in the precursor solution have been proven to be able to control the growth orientation and crystallinity of 2D RP perovskites. Some additives can be removed during the thermal annealing process. The interaction between the additive and the molecules or ions in the precursor solution changes the crystal growth and orientation. For instance, the vertical orientation of $(PEA)_2(MA)_{n-1}PbnI_{3n+1}$ (n = 3, 4, 5) 2D RP films was achieved by adding NH_4SCN to the precursor solution, i.e., the coordination bond between SCN^- and Pb^{2+} promoted the growth of the vertical orientation structure [81]. Moreover, the additive mixture of NH_4SCN and NH_4Cl has been introduced to obtain the vertical orientation of the $(PEA)_2(MA)_4Pb_5I_{16}$ film [82]. These two additives induced crystal growth in the vertical direction of the substrate and improved the crystallinity of the film. In particular, Cl^- (provided by NH_4Cl) effectively passivates the electron traps, which improves the open-circuit voltage (V_{OC}) of solar cells. Huang *et al.* [83] reported the introduction of methylammonium chloride (MACl) additives to prepare high-quality 2D RP perovskite films with vertical growth orientation. Because of the coordination between PbI_2 and MACl, the crystalline precursor was formed in the precursor solution, which is perpendicular to the substrate (Fig. 4(a)). Although MACl was volatilized after the annealing process, the vertical orientation structure was still preserved in the 2D RP perovskite film. In particular, the crystallization of the 2D RP perovskite phase with a small n value can be induced by the addition of MACl to the precursor solution (Fig. 4(b)) [84]. Then, the 2D RP perovskite phase with a large n value with vertical orientation crystals can be obtained. The oriented 2D RP perovskite films can be prepared by applying the *N*,*N*-dimethylformamide (DMF)/dimethyl sulfoxide (DMSO) mixed solvent process [85]. The results show that the strong hydrogen bond between polarized DMSO and organic cation reduces the crystal growth rate to facilitate the crystal orientation growth of 2D RP perovskites. The composition of the solvent has a considerable effect on the crystal orientation of 2D RP perovskites [86]. Compared with DMF and DMSO, dimethylacetamide (DMAC) has a moderate boiling point, low polarity, and weak coordination with lead and ammonium salts. DMAC is easily volatilized during the spin-coating process, accelerating the crystallization rate of 2D RP perovskite. The 2D RP perovskite films with DMAC exhibit a better crystal orientation compared with DMF and DMSO.

The partial substitution of some A-site organic ions has improved the crystal quality and growth orientation of 2D RP perovskite films. For example, Cs^+, one of the A-site inorganic ions, has improved the crystal quality of 2D RP perovskite films. The results show that the introduction of Cs^+ could improve the crystal orientation and prolong the crystallization kinetics of 2D RP perovskites to increase the grain

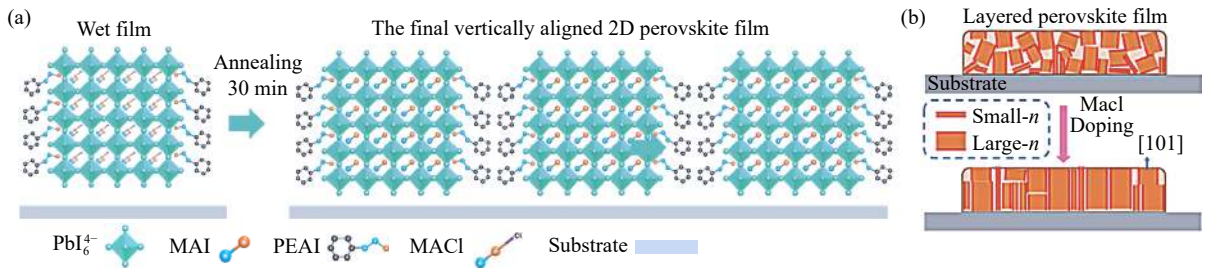

Fig. 4. (a) Schematic of the growth process of the vertically aligned 2D RP perovskite by adding MACl. Reprinted from *Chem. Eng. J.*, 394, F. Huang, P. Siffalovic, B. Li, S.X. Yang, L.X. Zhang, P. Nadazdy, G.Z. Cao, and J.J. Tian, Controlled crystallinity and morphologies of 2D Ruddlesden-Popper perovskite films grown without anti-solvent for solar cells, 124959, Copyright 2020, with permission from Elsevier. (b) Schematic of the phase orientation variation of the layered perovskite films with the addition of MACl. Reprinted with permission from Ref. [84]. Copyright 2020 American Chemical Society.

size [87]. The introduction of FA^+ can also control the 2D RP perovskite crystallization and crystal orientation [88]. This capability can be attributed to the interaction between FA^+ and I^-, which promotes the growth of a small *n* value perovskite phase.

4.2. Organic spacer cations

The optoelectronic performance of 2D RP perovskites could be improved by introducing functional groups to modify organic spacer cations. For example, a spacer cation of 4-fluoro-phenethylammonium (4FPEA) was used to fabricate 2D RP perovskite films [89]. The 4FPEA cation contains fluorine atoms that have a strong dipole field to facilitate charge separation of 2D RP perovskites. The *para*-substitution of fluorine may reduce the disorder in the structure, thus improving the crystallinity and vertical crystallization orientation of 2D RP perovskites. Sulfur atoms are also introduced into some organic cations, e.g., 2-(methylthio)ethylamine hydrochloride (MTEACl) [90]. The 2D RP perovskite films with MTEACl as spacer cation exhibit clearer and more discrete Bragg spots than 3D perovskite and BA-based films, indicating the oriented structure (Fig. 5(a)–(c)). This finding is attributed to the strong interaction between interlayer molecules because of the presence of sulfur–sulfur (S-S) interaction, which is expected to fix the framework of the 2D RP perovskite phase to assist the vertical growth of perovskite

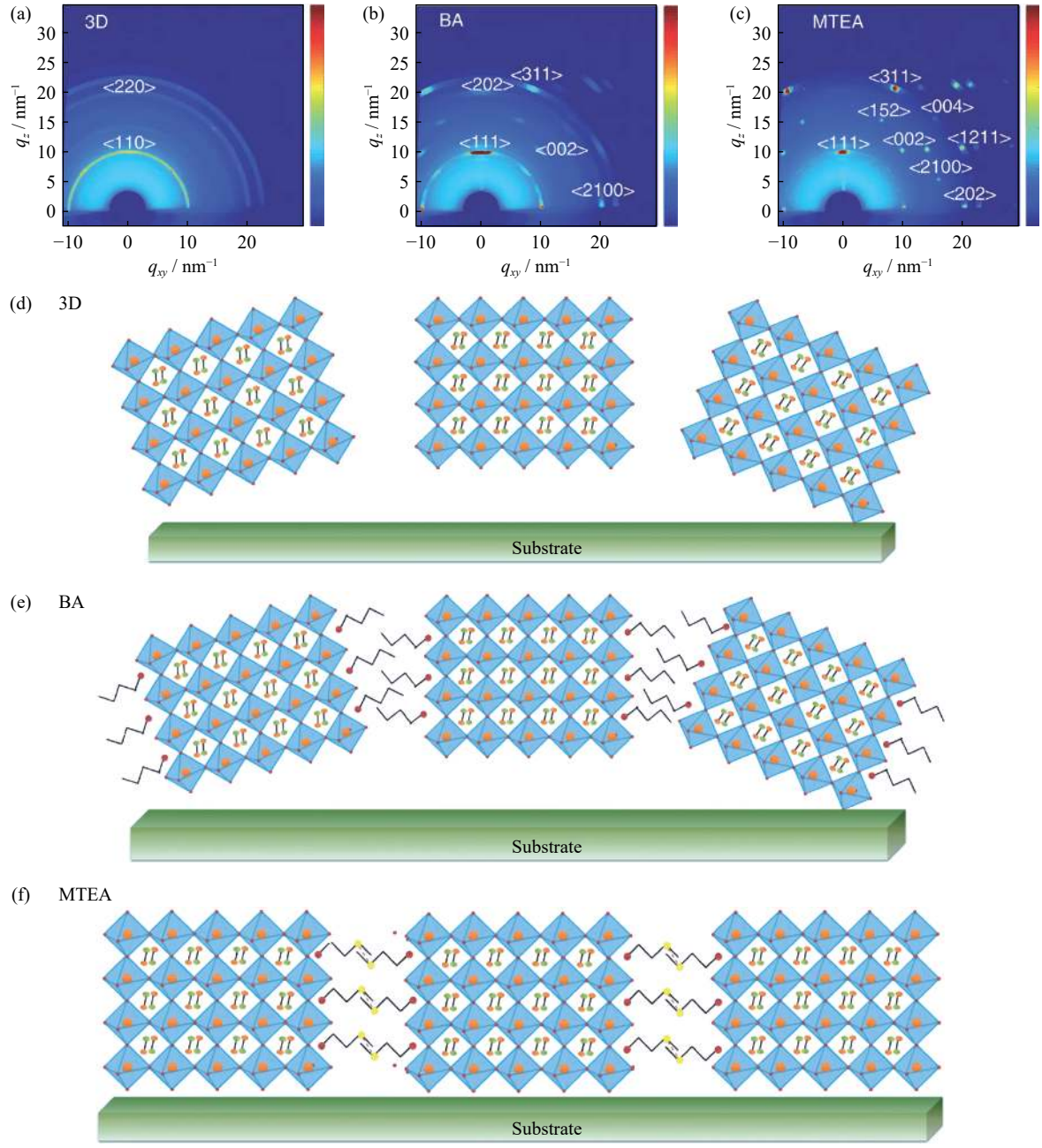

Fig. 5. GIWAXS patterns of (a) 3D, (b) BA-based, and (c) MTEA-based perovskite films. The color bars represent the diffraction intensity. Schematic illustrations of (d) 3D, (e) BA-based, and (f) MTEA-based perovskite films from random to vertical orientation. Reprinted by permission from Spring Nature: *Nat. Photonics*, Efficient and stable Ruddlesden–Popper perovskite solar cell with tailored interlayer molecular interaction, H. Ren, S.D. Yu, L.F. Chao, *et al.*, Copyright 2020.

crystals (Fig. 5(d)–(f)). The first principle calculations have confirmed the S-S interaction between two 2-(methylthio) ethylamine groups. Moreover, the S-S interaction ensures that the 2D RP perovskite films exhibit out-of-plane preferred crystal growth and orientation and helps form smooth and compact high-quality films. When the long-chain butylamine (BA) cation was converted into short branched-chain butylamine (iso-BA) spacer cation, iso-BA could improve the crystallinity and growth orientation of 2D RP perovskite films [91]. The nonlinear structure of the spacer organic cation resulted in the strong out-of-plane growth orientation of the $(iso\text{-}BA)_2(MA)_3Pb_4I_{13}$ film because the branched-chain spacers increased the orderly arrangement in the crystal. Furthermore, the mixture of PEA and BA as spacer cation was used to prepare 2D RP perovskites [92]. In the mixture film, the long-chain BA promoted the assembly of the oriented structure, whereas PEA doping preserved the original structure. The density functional theory calculations showed that the exciton binding energy in the mixed 2D RP perovskites, which results in the interaction between π-electrons (PEA^+) and I^- from Pb_6^{4-}, could be effectively reduced. Recently, a pure-phase 2D RP perovskite film with single-well width was obtained using *n*-butylamine acetate (BAAc) instead of *n*-butylamine iodide (BAI) [93]. The strong interaction between Ac^- and Pb^{2+} in perovskites might prevent the aggregation of colloid particles and induce the vertical orientation of grain growth crystallization. A comparison of the films deposited with BAI and BAAc by femtosecond transient absorption measurements showed that single photobleaching peaks were dominant in 2D RP films prepared using BAAc. Grazing-incidence wide-angle X-ray scattering (GIWAXS) measurements also showed that the films with BAAc exhibited better crystallinity and preferred orientation compared with traditional halide spacer.

5. Conclusion and outlook

The 2D RP perovskite has a sandwich structure in which both sides of the perovskite octahedral layer are surrounded by organic spacer cations. The unique structure of 2D RP perovskite has special requirements for its growth orientation. Considering that the conduction of charge carriers is limited by the organic spacer cations in the 2D RP perovskite layer, the orientation of 2D RP perovskites plays an important role in charge collection and transport. For example, if the growth orientation of the 2D RP perovskite is parallel to the substrate, the charge transfer would be hindered, reducing the device performance. Controlling the crystallographic growth orientation of 2D RP perovskites was considered important for improving the performance of solar cells. From the manufacturing process, the early one-step spin-coating method has gradually developed into the hot-casting, vacuum poling, and SVA methods. The hot-casting method controls the growth orientation of the 2D perovskite film by accelerating the transformation of the intermediate phase. Meanwhile, the SVA method uses solvent vapor to induce phase reorganization. The additive and organic spacer cations mainly affect the growth direction of the 2D RP perovskite crystal through the interaction between the functional group and the perovskite octahedron. Therefore, appropriate processes and additives should be used to obtain high-performance PSCs. Recently, the PCE of 2D RP PSCs has reached more than 18%.

To date, there is still a large room for 2D RP perovskites to reach the efficiency of 3D PSCs. First, the organic spacer cations usually exhibit low conductivity, limiting the charge transfer and reducing the short-circuit current of devices. Cations from different functional groups exhibit different physical and chemical properties; thus, the organic spacer cations should be carefully modified to balance the efficiency and stability of photovoltaic devices. The organic spacer cations of the 2D RP perovskite are staggered between adjacent layers, which is detrimental to the structural stability and carrier transport between adjacent layers. By contrast, in 2D DJ perovskites, the organic spacer cations are connected to the adjacent octahedral layer framework, which may improve the structural stability and charge transfer. Second, the 2D RP perovskite phase was a heterogeneous blend structure, and the phase distribution with different *n* values was uniform. Therefore, controlling the phase composition and distribution is important to improve the performance of PSCs. Finally, the introduction of a large volume of organic spacer cations would result in lattice structure deformation, which causes the dielectric mismatch of 2D RP perovskite structures. The 3D phase could be epitaxially grown on 2D grain boundaries, and the 2D/3D interface problem could be introduced. Although the performance of 2D RP perovskites has been improved, the corresponding formation mechanism and modification process are still unclear. Thus, further investigations are necessary for an in-depth understanding of the mechanism of 2D PR perovskites. Moreover, the application of 2D PR perovskites in the photovoltaic area needs to be investigated.

Acknowledgements

This work was financially supported by the National Key Research and Development Program of China (No. 2017YFE0119700) and the National Natural Science Foundation of China (Nos. 51961135107, 51774034, and 5177 2026).

Conflict of Interest

The authors declared that they have no conflicts of interest.

References

[1] F. Huang, M.J. Li, P. Siffalovic, G.Z. Cao, and J.J. Tian, From scalable solution fabrication of perovskite films towards commercialization of solar cells, *Energy Environ. Sci.*, 12(2019), No. 2, p. 518.

[2] A.Q. Liu, C.H. Bi, R.Q. Guo, M.Q. Zhang, X.H. Qu, and J.J.

Tian, Electroluminescence principle and performance improvement of metal halide perovskite light-emitting diodes, *Adv. Opt. Mater.*, 9(2021), No. 18, art. No. 2002167.
[3] H. Kim, K.G. Lim, and T.W. Lee, Planar heterojunction organometal halide perovskite solar cells: Roles of interfacial layers, *Energy Environ. Sci.*, 9(2016), No. 1, p. 12.
[4] C.H. Bi, Z.W. Yao, X.J. Sun, X.C. Wei, J.X. Wang, and J.J. Tian, Perovskite quantum dots with ultralow trap density by acid etching-driven ligand exchange for high luminance and stable pure-blue light-emitting diodes, *Adv. Mater.*, 33(2021), No. 15, art. No. 2006722.
[5] C.F. Liu, J.F. Yuan, R. Masse, *et al*., Interphases, interfaces, and surfaces of active materials in rechargeable batteries and perovskite solar cells, *Adv. Mater.*, 33(2021), No. 22, art. No. 1905245.
[6] V. D'Innocenzo, G. Grancini, M.J.P. Alcocer, *et al*., Excitons versus free charges in organo-lead tri-halide perovskites, *Nat. Commun.*, 5(2014), art. No. 3586.
[7] B. Li, D. Binks, G.Z. Cao, and J.J. Tian, Engineering halide perovskite crystals through precursor chemistry, *Small*, 15(2019), No. 47, art. No. 1903613.
[8] C.H. Bi, X.J. Sun, X. Huang, *et al*., Stable $CsPb_{1-x}Zn_xI_3$ colloidal quantum dots with ultralow density of trap states for high-performance solar cells, *Chem. Mater.*, 32(2020), No. 14, p. 6105.
[9] T. Yang, Y.P. Zheng, K.C. Chou, and X.M. Hou, Tunable fabrication of single-crystalline $CsPbI_3$ nanobelts and their application as photodetectors, *Int. J. Miner. Metall. Mater.*, 28(2021), No. 6, p. 1030.
[10] D.W. De Quilettes, S.M. Vorpahl, S.D. Stranks, *et al*, Impact of microstructure on local carrier lifetime in perovskite solar cells, *Science*, 348(2015), No. 6235, p. 683.
[11] J.H. Zheng, L.X. Zhu, Z.T. Shen, *et al*., Effects of the incorporation amount of CdS and $Cd(SCN_2H_4)_2Cl_2$ on the performance of perovskite solar cells, *Int. J. Miner. Metall. Mater.*, (2021). DOI:10.1007/s12613-021-2316-0
[12] D. Zhang, J.F. Yuan, and J.J. Tian, All-inorganic perovskite solar cells with efficiency >20%, *Sci. China Mater.*, 64(2021), No. 10, p. 2624.
[13] H.Y. Zhang, R. Li, W.W. Liu, M. Zhang, and M. Guo, Research progress in lead-less or lead-free three-dimensional perovskite absorber materials for solar cells, *Int. J. Miner. Metall. Mater.*, 26(2019), No. 4, p. 387.
[14] D. Weber, $CH_3NH_3PbX_3$, ein Pb(II)-system mit kubischer perowskitstruktur / $CH_3NH_3PbX_3$, a Pb(II)-system with cubic perovskite structure, *Z. Naturforsch. B*, 33(1978), No. 12, p. 1443.
[15] A. Kojima, K. Teshima, Y. Shirai, and T. Miyasaka, Organometal halide perovskites as visible-light sensitizers for photovoltaic cells, *J. Am. Chem. Soc.*, 131(2009), No. 17, p. 6050.
[16] H.S. Kim, C.R. Lee, J.H. Im, *et al*., Lead iodide perovskite sensitized all-solid-state submicron thin film mesoscopic solar cell with efficiency exceeding 9%, *Sci. Rep.*, 2(2012), art. No. 591.
[17] X.Z. Yu, Y. Qin, and Q. Peng, Probe decomposition of methylammonium lead iodide perovskite in N_2 and O_2 by *in situ* infrared spectroscopy, *J. Phys. Chem. A*, 121(2017), No. 6, p. 1169.
[18] Y.P. Xia, P.H. Wang, S.W. Shi, *et al*., Effect of oxygen partial pressure and transparent substrates on the structural and optical properties of ZnO thin films and their performance in energy harvesters, *Int. J. Miner. Metall. Mater.*, 24(2017), No. 6, p. 675.
[19] G. Tumen-Ulzii, C.J. Qin, D. Klotz, *et al*., Detrimental effect of unreacted PbI_2 on the long-term stability of perovskite solar cells, *Adv. Mater.*, 32(2020), No. 16, art. No. 1905035.
[20] H.T. Wei, S.S. Chen, J.J. Zhao, Z.H. Yu, and J.S. Huang, Is formamidinium always more stable than methylammonium?, *Chem. Mater.*, 32(2020), No. 6, p. 2501.
[21] L. McGovern, I. Koschany, G. Grimaldi, L.A. Muscarella, and B. Ehrler, Grain size influences activation energy and migration pathways in $MAPbBr_3$ perovskite solar cells, *J. Phys. Chem. Lett.*, 12(2021), No. 9, p. 2423.
[22] P. Chen, Y. Bai, S.C. Wang, M.Q. Lyu, J.H. Yun, and L.Z. Wang, *In situ* growth of 2D perovskite capping layer for stable and efficient perovskite solar cells, *Adv. Funct. Mater.*, 28(2018), No. 17, art. No. 1706923.
[23] J. Zhuang, P. Mao, Y.G. Luan, *et al*., Interfacial passivation for perovskite solar cells: The effects of the functional group in phenethylammonium iodide, *ACS Energy Lett.*, 4(2019), No. 12, p. 2913.
[24] C.L. Zhang, S.H. Wu, L.M. Tao, *et al*., Fabrication strategy for efficient 2D/3D perovskite solar cells enabled by diffusion passivation and strain compensation, *Adv. Energy Mater.*, 10(2020), No. 43, art. No. 2002004.
[25] Y.H. Wu, Y. Ding, X.Y. Liu, *et al*., Ambient stable $FAPbI_3$-based perovskite solar cells with a 2D-$EDAPbI_4$ thin capping layer, *Sci. China Mater.*, 63(2020), No. 1, p. 47.
[26] H.Y. Zheng, S.Y. Dai, K.X. Zhou, *et al*., New-type highly stable 2D/3D perovskite materials: The effect of introducing ammonium cation on performance of perovskite solar cells, *Sci. China Mater.*, 62(2019), No. 4, p. 508.
[27] Y.H. Liu, S. Akin, A. Hinderhofer, *et al*., Stabilization of highly efficient and stable phase-pure $FAPbI_3$ perovskite solar cells by molecularly tailored 2D-overlayers, *Angew. Chem. Int. Ed.*, 59(2020), No. 36, p. 15688.
[28] C.T. Zuo, A.D. Scully, W.L. Tan, *et al*, Crystallisation control of drop-cast quasi-2D/3D perovskite layers for efficient solar cells, *Commun. Mater.*, 1(2020), art. No. 33.
[29] Y. Li, J.V. Milić, A. Ummadisingu, *et al*, Bifunctional organic spacers for formamidinium-based hybrid Dion−Jacobson two-dimensional perovskite solar cells, *Nano Lett.*, 19(2019), No. 1, p. 150.
[30] B.E. Cohen, Y.M. Li, Q.B. Meng, and L. Etgar, Dion−Jacobson two-dimensional perovskite solar cells based on benzene dimethanammonium cation, *Nano Lett.*, 19(2019), No. 4, p. 2588.
[31] F.Z. Li, J. Zhang, S.B. Jo, *et al*., Vertical orientated Dion−Jacobson quasi-2D perovskite film with improved photovoltaic performance and stability, *Small Methods*, 4(2020), No. 5, art. No. 1900831.
[32] D. Lu, G.W. Lv, Z.Y. Xu, Y.X. Dong, X.F. Ji, and Y.S. Liu, Thiophene-based two-dimensional Dion−Jacobson perovskite solar cells with over 15% efficiency, *J. Am. Chem. Soc.*, 142(2020), No. 25, p. 11114.
[33] H.T. Wu, X.M. Lian, S.X. Tian, *et al*., Additive assisted hot-casting free fabrication of Dion-Jacobson 2D perovskite solar cell with efficiency beyond 16%, *Sol. RRL*, 4(2020), No. 7, art. No. 2000087.
[34] W.D. Zhao, Q.S. Dong, J.W. Zhang, *et al*., Asymmetric alkyl diamine based Dion–Jacobson low-dimensional perovskite solar cells with efficiency exceeding 15%, *J. Mater. Chem. A*, 8(2020), No. 19, p. 9919.
[35] H. Wang, Z.T. Qin, J.S. Xie, *et al*., Efficient slantwise aligned Dion−Jacobson phase perovskite solar cells based on trans-1, 4-cyclohexanediamine, *Small*, 16(2020), No. 42, art. No. 2003098.
[36] J. Kim, W. Lee, K. Cho, *et al*., Crystallinity-dependent device characteristics of polycrystalline 2D $n = 4$ Ruddlesden–Popper perovskite photodetectors, *Nanotechnol.*, 32(2021), No. 18, art. No. 185203.
[37] B. Hwang, Y. Park, and J.S. Lee, Impact of grain size on the optoelectronic performance of 2D Ruddlesden–Popper perovskite-based photodetectors, *J. Mater. Chem. C*, 9(2021), No. 1, p. 110.
[38] G. Jang, S. Ma, H.C. Kwon, *et al*., Elucidation of the formation mechanism of highly oriented multiphase Ruddlesden–Popper perovskite solar cells, *ACS Energy Lett.*, 6(2021), No. 1, p. 249.
[39] J.S. Shi, X. Jin, Y.Z. Wu, and M. Shao, Mixed bulky cations for

efficient and stable Ruddlesden−Popper perovskite solar cells, *APL Mater.*, 8(2020), No. 10, art. No. 101102.
[40] X.L. Tang, X.Y. Wang, T. Hu, *et al*., Concerted regulation on vertical orientation and film quality of two-dimensional Ruddlesden−Popper perovskite layer for efficient solar cells, *Sci. China Chem.*, 63(2020), No. 11, p. 1675.
[41] J.M. Yang, S.B. Xiong, J.N. Song, *et al*., Energetics and energy loss in 2D Ruddlesden−Popper perovskite solar cells, *Adv. Energy Mater.*, 10(2020), No. 23, art. No. 2000687.
[42] Y. Qin, H.J. Zhong, J.J. Intemann, *et al*., Coordination engineering of single-crystal precursor for phase control in Ruddlesden−Popper perovskite solar cells, *Adv. Energy Mater.*, 10(2020), No. 16, art. No. 1904050.
[43] S.N. Ruddlesden and P. Popper, New compounds of the K_2NIF_4 type, *Acta Cryst.*, 10(1957), No. 8, p. 538.
[44] I.C. Smith, E.T. Hoke, D. Solis-Ibarra, M.D. McGehee, and H.I. Karunadasa, A layered hybrid perovskite solar-cell absorber with enhanced moisture stability, *Angew. Chem. Int. Ed.*, 53(2014), No. 42, p. 11232.
[45] T. Zhang, M.I. Dar, G. Li, *et al*., Bication lead iodide 2D perovskite component to stabilize inorganic α-$CsPbI_3$ perovskite phase for high-efficiency solar cells, *Sci. Adv.*, 3(2017), No. 9, art. No. e1700841.
[46] L. Etgar, The merit of perovskite's dimensionality; can this replace the 3D halide perovskite, *Energy Environ. Sci.*, 11(2018), No. 2, p. 234.
[47] S. Yang, Y. Wang, P.R. Liu, Y.B. Cheng, H.J. Zhao, and H.G. Yang, Functionalization of perovskite thin films with moisture-tolerant molecules, *Nat. Energy*, 1(2016), art. No. 15016.
[48] H.J. Jung, C.C. Stompus, M.G. Kanatzidis, and V.P. Dravid, Self-passivation of 2D Ruddlesden–Popper perovskite by polytypic surface PbI_2 encapsulation, *Nano Lett.*, 19(2019), No. 9, p. 6109.
[49] Y. Lin, Y. Bai, Y.J. Fang, Q. Wang, Y.H. Deng, and J.S. Huang, Suppressed ion migration in low-dimensional perovskites, *ACS Energy Lett.*, 2(2017), No. 7, p. 1571.
[50] G.B. Wu, T.H. Yang, X. Li, *et al*., Molecular engineering for two-dimensional perovskites with photovoltaic efficiency exceeding 18%, *Matter*, 4(2021), No. 2, p. 582.
[51] R. Yang, R.Z. Li, Y. Cao, *et al*, Oriented quasi-2D perovskites for high performance optoelectronic devices, *Adv. Mater.*, 30(2018), No. 51, art. No. 1804771.
[52] Y. Yang, C. Liu, O.A. Syzgantseva, *et al*., Defect suppression in oriented 2D perovskite solar cells with efficiency over 18% via rerouting crystallization pathway, *Adv. Energy Mater.*, 11(2021), No. 1, art. No. 2002966.
[53] H.T. Lai, D. Lu, Z.Y. Xu, N. Zheng, Z.Q. Xie, and Y.S. Liu, Organic-salt-assisted crystal growth and orientation of quasi-2D Ruddlesden−Popper perovskites for solar cells with efficiency over 19%, *Adv. Mater.*, 32(2020), No. 33, art. No. 2001470.
[54] D.H. Cao, C.C. Stoumpos, O.K. Farha, J.T. Hupp, and M.G. Kanatzidis, 2D homologous perovskites as light-absorbing materials for solar cell applications, *J. Am. Chem. Soc.*, 137(2015), No. 24, p. 7843.
[55] J.Z. Li, J. Wang, Y.J. Zhang, *et al*., Fabrication of single phase 2D homologous perovskite microplates by mechanical exfoliation, *2D Mater.*, 5(2018), No. 2, art. No. 021001.
[56] L.N. Quan, M.J. Yuan, R. Comin, *et al*., Ligand-stabilized reduced-dimensionality perovskites, *J. Am. Chem. Soc.*, 138(2016), No. 8, p. 2649.
[57] C.C. Stoumpos, D.H. Cao, D.J. Clark, *et al*., Ruddlesden–Popper hybrid lead iodide perovskite 2D homologous semiconductors, *Chem. Mater.*, 28(2016), No. 8, p. 2852.
[58] W.J. Wei, X.X. Jiang, L.Y. Dong, *et al*., Regulating second-harmonic generation by van der Waals interactions in two-dimensional lead halide perovskite nanosheets, *J. Am. Chem. Soc.*, 141(2019), No. 23, p. 9134.
[59] X. Hong, T. Ishihara, and A.V. Nurmikko, Dielectric confinement effect on excitons in PbI_4-based layered semiconductors, *Phys. Rev. B*, 45(1992), No. 12, p. 6961.
[60] D.H. Cao, C.C. Stoumpos, T. Yokoyama, *et al*., Thin films and solar cells based on semiconducting two-dimensional Ruddlesden–Popper $(CH_3(CH_2)_3NH_3)_2(CH_3NH_3)_{n-1}Sn_nI_{3n+1}$ perovskites, *ACS Energy Lett.*, 2(2017), No. 5, p. 982.
[61] A.Z. Chen, M. Shiu, J.H. Ma, *et al*, Origin of vertical orientation in two-dimensional metal halide perovskites and its effect on photovoltaic performance, *Nat. Commun.*, 9(2018), art. No. 1336.
[62] M. Konstantakou, D. Perganti, P. Falaras, and T. Stergiopoulos, Anti-solvent crystallization strategies for highly efficient perovskite solar cells, *Crystals*, 7(2017), No. 10, art. No. 291.
[63] M. Zhang, Z.H. Wang, B. Zhou, *et al*., Green anti-solvent processed planar perovskite solar cells with efficiency beyond 19%, *Sol. RRL*, 2(2018), No. 2, art. No. 1700213.
[64] Y.F. Wang, J. Wu, P. Zhang, *et al*., Stitching triple cation perovskite by a mixed anti-solvent process for high performance perovskite solar cells, *Nano Energy*, 39(2017), p. 616.
[65] D. Prochowicz, M.M. Tavakoli, A. Solanki, *et al*., Understanding the effect of chlorobenzene and isopropanol anti-solvent treatments on the recombination and interfacial charge accumulation in efficient planar perovskite solar cells, *J. Mater. Chem. A*, 6(2018), No. 29, p. 14307.
[66] Y. Li, J.A. Wang, Y. Yuan, X.D. Dong, and P. Wang, Anti-solvent dependent device performance in $CH_3NH_3PbI_3$ solar cells: The role of intermediate phase content in the as-prepared thin films, *Sustainable Energy Fuels*, 1(2017), No. 5, p. 1041.
[67] Y.X. Dong, D. Lu, Z.Y. Xu, H.T. Lai, and Y.S. Liu, 2-thiopheneformamidinium-based 2D Ruddlesden-Popper perovskite solar cells with efficiency of 16.72% and negligible hysteresis, *Adv. Energy Mater.*, 10(2020), No. 28, art. No. 2000694.
[68] M.J. Li, B. Li, G.Z. Cao, and J.J. Tian, Monolithic $MAPbI_3$ films for high-efficiency solar cells via coordination and a heat assisted process, *J. Mater. Chem. A*, 5(2017), No. 40, p. 21313.
[69] H.C. Liao, P.J. Guo, C.P. Hsu, *et al*., Enhanced efficiency of hot-cast large-area planar perovskite solar cells/modules having controlled chloride incorporation, *Adv. Energy Mater.*, 7(2017), No. 8, art. No. 1601660.
[70] W.Y. Nie, H. Tsai, R. Asadpour, *et al*., High-efficiency solution-processed perovskite solar cells with millimeter-scale grains, *Science*, 347(2015), No. 6221, p. 522.
[71] Z. Wang, X.D. Liu, Y.W. Lin, *et al*, Hot-substrate deposition of all-inorganic perovskite films for low-temperature processed high-efficiency solar cells, *J. Mater. Chem. A*, 7(2019), No. 6, p. 2773.
[72] G.B. Wu, J.Y. Zhou, J.Q. Zhang, *et al*, Management of the crystallization in two-dimensional perovskite solar cells with enhanced efficiency within a wide temperature range and high stability, *Nano Energy*, 58(2019), p. 706.
[73] G.S. Shin, W.G. Choi, S. Na, F.P. Gökdemir, and T. Moon, Lead acetate based hybrid perovskite through hot casting for planar heterojunction solar cells, *Electron. Mater. Lett.*, 14(2018), No. 2, p. 155.
[74] H. Tsai, W.Y. Nie, J.C. Blancon, *et al*, High-efficiency two-dimensional Ruddlesden-Popper perovskite solar cells, *Nature*, 536(2016), No. 7616, p. 312.
[75] F.D. Wang, Y.Y. Wang, Y.H. Liu, P.J. Morrison, R.A. Loomis, and W.E. Buhro, Two-dimensional semiconductor nanocrystals: Properties, templated formation, and magic-size nanocluster intermediates, *Acc. Chem. Res.*, 48(2015), No. 1, p. 13.
[76] A. Riedinger, F.D. Ott, A. Mule, *et al*., An intrinsic growth instability in isotropic materials leads to quasi-two-dimensional nanoplatelets, *Nat. Mater.*, 16(2017), No. 7, p. 743.
[77] R. Quintero-Bermudez, A. Gold-Parker, A.H. Proppe, *et al*., Compositional and orientational control in metal halide perovskites of reduced dimensionality, *Nat. Mater.*, 17(2018), No. 10, p. 900.
[78] S.Y. Shao, H. Duim, Q.Q. Wang, *et al*., Tuning the energetic

landscape of Ruddlesden−Popper perovskite films for efficient solar cells, *ACS Energy Lett.*, 5(2020), No. 1, p. 39.
[79] J. Zhang, J.J. Qin, M.S. Wang, *et al*., Uniform permutation of quasi-2D perovskites by vacuum poling for efficient, high-fill-factor solar cells, *Joule*, 3(2019), No. 12, p. 3061.
[80] X.M. Zhao, T.R. Liu, A.B. Kaplan, C. Yao, and Y.L. Loo, Accessing highly oriented two-dimensional perovskite films via solvent-vapor annealing for efficient and stable solar cells, *Nano Lett.*, 20(2020), No. 12, p. 8880.
[81] X.Q. Zhang, G. Wu, W.F. Fu, *et al*., Orientation regulation of phenylethylammonium cation based 2D perovskite solar cell with efficiency higher than 11%, *Adv. Energy Mater.*, 8(2018), No. 14, art. No. 1702498.
[82] W.F. Fu, J. Wang, L.J. Zuo, *et al*., Two-dimensional perovskite solar cells with 14.1% power conversion efficiency and 0.68% external radiative efficiency, *ACS Energy Lett.*, 3(2018), No. 9, p. 2086.
[83] F. Huang, P. Siffalovic, B. Li, *et al*., Controlled crystallinity and morphologies of 2D Ruddlesden−Popper perovskite films grown without anti-solvent for solar cells, *Chem. Eng. J.*, 394(2020), art. No. 124959.
[84] F. Zheng, C.T. Zuo, M.S. Niu, *et al*., Revealing the role of methylammonium chloride for improving the performance of 2D perovskite solar cells, *ACS Appl. Mater. Interfaces*, 12(2020), No. 23, p. 25980.
[85] C.M.M. Soe, W.Y. Nie, C.C. Stoumpos, *et al*., Understanding film formation morphology and orientation in high member 2D Ruddlesden–Popper perovskites for high-efficiency solar cells, *Adv. Energy Mater.*, 8(2018), No. 1, art. No. 1700979.
[86] J. Qiu, Y.T. Zheng, Y.D. Xia, *et al*., Rapid crystallization for efficient 2D Ruddlesden–Popper (2DRP) perovskite solar cells, *Adv. Funct. Mater.*, 29(2019), No. 47, art. No. 1806831.
[87] X. Zhang, X.D. Ren, B. Liu, *et al*., Stable high efficiency two-dimensional perovskite solar cells via cesium doping, *Energy Environ. Sci.*, 10(2017), No. 10, p. 2095.
[88] N. Zhou, Y.H. Shen, L. Li, *et al*., Exploration of crystallization kinetics in quasi two-dimensional perovskite and high performance solar cells, *J. Am. Chem. Soc.*, 140(2018), No. 1, p. 459.
[89] J.S. Shi, Y.R. Gao, X. Gao, *et al*., Fluorinated low-dimensional Ruddlesden−Popper perovskite solar cells with over 17% power conversion efficiency and improved stability, *Adv. Mater.*, 31(2019), No. 37, art. No. 1901673.
[90] H. Ren, S.D. Yu, L.F. Chao, *et al*., Efficient and stable Ruddlesden–Popper perovskite solar cell with tailored interlayer molecular interaction, *Nat. Photonics*, 14(2020), No. 3, p. 154.
[91] Y.N. Chen, Y. Sun, J.J. Peng, *et al*., Tailoring organic cation of 2D air-stable organometal halide perovskites for highly efficient planar solar cells, *Adv. Energy Mater.*, 7(2017), No. 18, art. No. 1700162.
[92] N. Zhou, B.L. Huang, M.Z. Sun, *et al*., The spacer cations interplay for efficient and stable layered 2D perovskite solar cells, *Adv. Energy Mater.*, 10(2020), No. 1, art. No. 1901566.
[93] C. Liang, H. Gu, Y.D. Xia, *et al*., Two-dimensional Ruddlesden–Popper layered perovskite solar cells based on phase-pure thin films, *Nat. Energy*, 6(2021), No. 1, p. 38.